Transmission and reflection of holes from barriers and wells in semiconductor heterostructures

1995 J. Phys.: Condens. Matter 7 2059

(http://iopscience.iop.org/0953-8984/7/10/013)

J. Phys.: Condens. Matter 7 (1995) 2059–2079. Printed in the UK

Transmission and reflection of holes from barriers and wells in semiconductor heterostructures

A D Sánchez and C R Proetto

Centro Atómico Bariloche and Instituto Balseiro, Comisión Nacional de Energía Atómica, 8400 Bariloche, Argentina

Received 16 September 1994, in final form 12 December 1994

Abstract. The quantum mechanical problem of tunnelling and reflection of holes from barriers and wells in semiconductor heterojunctions has been analysed. By using the Luttinger Hamiltonian to describe the dynamics of holes, the inherent anisotropy, non-parabolicity and heavy- and light-hole mixing at the top of the valence band has been taken into account. The symmetries of the hole scattering matrix are worked out, from which very general relations among the reflectivities and transmissivities are obtained. These analytical results are complemented by numerical calculations for several different situations; within the range of parameters investigated, no resonant unity transmission above the barrier is found. We do find that the transmission is zero (anti-resonances) in the well configuration for particular values of the energy of the incoming heavy hole.

1. Introduction

Tunnelling and reflection from one-dimensional square barriers and wells are traditional problems of quantum mechanics; however, for several decades they were considered instructive but essentially academic idealizations of real physical systems. With the arrival of the manufactured semiconductor heterostructures, these problems became also of practical interest, as the epitaxial growth heterointerface between two different semiconductors is almost an ideal realization of a step potential. Among the many unexpected results that these systems produce in the field of basic physics one might mention the integer [1] and fractional [2] quantum Hall effect, the unambiguous observation of Wannier–Stark ladders in superlattices [3], and the quantization of the electrical conductance in quantum-point contacts [4, 5]. On the other hand, the interest comes also as a consequence of their potential applications in electronic (for instance, resonant tunnelling diodes) and optoelectronic (for instance, quantum-well lasers) devices.

Many theoretical methods have been applied to study their band structure, electronic and optical properties [6]. These methods can be divided into two general classes: the super-cell approach in which the heterostructure is viewed as a material with a large unit cell [7], and the boundary-condition approach in which bulk wave functions for each of the constituent semiconductors are matched at the heterostructure interfaces [8, 9]. Within the latter category, the envelope-function approach, based on the effective-mass approximation [10], is easy to apply; besides, it is particularly suited to including external perturbations, such as electric and magnetic fields, and uniaxial stress.

While experiments concerned with the electronic and optical properties of electrons in III–V compound semiconductors at the bottom of the conduction band can be usually

0953-8984/95/102059+21$19.50

described assuming a parabolic and isotropic dispersion relation, the situation for holes is more involved. As a consequence of the degeneracy at the top of the valence band, one is forced to use a multiband effective-mass theory, that in the case of GaAs–$Al_xGa_{1-x}As$ implies the use of the 4×4 Luttinger Hamiltonian [11], at least for energies smaller than the bottom of the Γ_7 spin-split-off doublet (~340 meV).

The aim of the present contribution is to generalize the well-known textbook results for the transmission and reflection of electrons by one-dimensional potentials to the case of holes described by the 4×4 Luttinger Hamiltonian. A first step in this direction has been made by Chuang [12], who considered the refraction holes at a single heterointerface (the equivalent of a step potential for electrons). In this work, we have extended these results to the case of refraction by potential barriers (including the case of a single heterointerface as a limiting case) and wells. Besides, this we include an analysis of the symmetries of the transmission and reflection coefficients, by making an extension of the one-channel scattering matrix formalism to a multi-channel case. The understanding of the dynamics of holes against simple obstacles such as barriers and wells is quite important, as they can be considered as the building blocks of more complicated devices, such as double-barrier resonant tunnelling systems and superlattices. Another situations where two or more pairs of states coexist at a given energy in a scattering process are: Γ–X mixing of electrons tunnelling through AlAs barriers [13, 14]; transmission across quasi-one dimensional systems [15]; and interband tunnelling [16, 17].

The scheme of calculation is similar to the one adopted by Andreani, Pasquarello and Bassani [18], Wessel and Altarelli [19], and Chao and Chuang [20] in their complementary study of the bounded-hole solutions of GaAs–$Ga_{1-x}Al_xAs$ quantum wells. We first solve the effective-mass equation in the well and barrier materials, and then match the bulk solutions at the heterointerfaces in order to find the eigenstates. The calculation scheme differs, however, in an important point: while the bulk solutions of [18] are linear combinations of four-component vectors, our use of a canonical transformation of the Luttinger Hamiltonian decouples it into two 2×2 blocks [21], and greatly simplifies the numerical calculation. A similar approach was used in [12].

From a more general perspective, the problem addressed in this paper can be considered as the simplest extension of the scattering matrix formalism, that usually considers only one type of propagating state in each region of space, to the case of two types of propagating states in each region of space (heavy and light holes). The connection with the scattering formalism proves to be quite useful, as it allows us to obtain quite general symmetry properties of the transmission and reflection coefficients.

The remaining part of the paper is organized as follows. We give in section 2 the canonical transformation which reduces the original 4×4 Luttinger Hamiltonian to two decoupled 2×2 blocks; we discuss the bulk solutions of each block, the definition of the probability current density, and also the corresponding boundary conditions that should be applied to match bulk solutions across each interface. In section 3 we discuss the general symmetries of the transmission and reflection coefficients, by making an extension of the scattering matrix formalism and using the time-reversal and spatial symmetries of the Hamiltonian. Section 4 is devoted to the numerical results, and there we present the transport coefficients both for the barrier and well cases. Finally, we give our conclusions in section 5.

2. Canonical transformation, hole wave functions, dispersion relations, probability currents and boundary conditions

We consider a potential barrier (well) of $Al_xGa_{1-x}As$ (GaAs) embedded in an otherwise homogeneous GaAs ($Al_xGa_{1-x}As$) host matrix, grown in a ⟨100⟩ direction, which we take along the quantization axis z. Due to translational symmetry in the (x, y) plane of our system, the envelope wave functions can be written as a plane wave along this plane times a wave function along z, the latter given by the solution of the following 4×4 block diagonalized effective-mass matrix Hamiltonian [21]:

$$\mathbf{H} = \begin{Vmatrix} P+Q & \tilde{R} & 0 & 0 \\ \tilde{R}^+ & P-Q & 0 & 0 \\ 0 & 0 & P-Q & \tilde{R} \\ 0 & 0 & \tilde{R}^+ & P+Q \end{Vmatrix} + V(z)\mathbf{I} \equiv \begin{pmatrix} \mathbf{H}^{\mathrm{U}} & 0 \\ 0 & \mathbf{H}^{\mathrm{L}} \end{pmatrix} + V(z)\mathbf{I} \tag{1}$$

where $V(z) = \pm\, \Delta E\, \theta(z)\theta(L-z)$ is the barrier (+) or well (−) potential (ΔE being the valence band offset), $\hat{k}_z$ is the operator $-\mathrm{i}\,\partial/\partial z$,

$$P \pm Q = \frac{\hbar^2}{2m}\left[(\gamma_1 \pm \gamma_2)(k_x^2 + k_y^2) + (\gamma_1 \mp 2\gamma_2)\hat{k}_z^2\right] \tag{2a}$$

$$R = \sqrt{3}\frac{\hbar^2}{2m}\left[\gamma_2(k_x^2 - k_y^2) - 2\mathrm{i}\gamma_3 k_x k_y\right] \tag{2b}$$

$$S = \sqrt{3}\frac{\hbar^2}{m}\gamma_3(k_x - \mathrm{i}k_y) \tag{2c}$$

$$\tilde{R} = |R| - \mathrm{i}\hat{k}_z|S| \tag{2d}$$

and the hole energy has been counted as positive. In equation (2) m is the free-electron mass, and $\gamma_1, \gamma_2, \gamma_3$ are the Luttinger parameters corresponding to the barrier or well and semi-infinite layer material. In writing the kinetic energy we have neglected very small linear k-terms caused by the lack of inversion symmetry of the zincblende structure [10].

The Hamiltonian (1) acts on a four-component envelope function

$$f(z) = \left[f_1(z),\ f_2(z),\ f_3(z),\ f_4(z)\right]$$

while the total electronic wave function is approximately given by

$$\begin{aligned}\psi(\boldsymbol{r}) &= \mathrm{e}^{\mathrm{i}(k_x x + k_y y)}\left[f_1(z)|1\rangle + f_2(z)|2\rangle + f_3(z)|3\rangle + f_4(z)|4\rangle\right] \\ &\equiv F_1(\boldsymbol{r})|1\rangle + F_2(\boldsymbol{r})|2\rangle + F_3(\boldsymbol{r})|3\rangle + F_4(\boldsymbol{r})|4\rangle.\end{aligned} \tag{3}$$

The states $|1\rangle$, $|2\rangle$, $|3\rangle$, and $|4\rangle$ which yield the block-diagonalized form of the Luttinger Hamiltonian are linear combinations of the usual Γ_8 Bloch functions $|J, J_z\rangle$ of both materials at $k = 0$, as follows:

$$\begin{aligned}|1\rangle &= \alpha\left|\frac{3}{2}, +\frac{3}{2}\right\rangle - \alpha^*\left|\frac{3}{2}, -\frac{3}{2}\right\rangle \\ |2\rangle &= \beta\left|\frac{3}{2}, -\frac{1}{2}\right\rangle - \beta^*\left|\frac{3}{2}, +\frac{1}{2}\right\rangle \\ |3\rangle &= \beta\left|\frac{3}{2}, -\frac{1}{2}\right\rangle + \beta^*\left|\frac{3}{2}, +\frac{1}{2}\right\rangle \\ |4\rangle &= \alpha\left|\frac{3}{2}, +\frac{3}{2}\right\rangle + \alpha^*\left|\frac{3}{2}, -\frac{3}{2}\right\rangle\end{aligned} \tag{4}$$

where α and β are chosen so that the Luttinger Hamiltonian in the new basis has the block-diagonalized form (1).

Following standard procedures we may represent schematically the total-angular-momentum states $|J, J_z\rangle$ using the space Bloch functions X, Y, Z and the spin functions $|\uparrow\rangle$ and $|\downarrow\rangle$

$$\begin{aligned}
\left|\frac{3}{2},+\frac{3}{2}\right\rangle &= -\frac{1}{\sqrt{2}}(X+\mathrm{i}Y)|\uparrow\rangle \\
\left|\frac{3}{2},-\frac{1}{2}\right\rangle &= \frac{1}{\sqrt{6}}(X-\mathrm{i}Y)|\uparrow\rangle + \sqrt{\frac{2}{3}}Z|\downarrow\rangle \\
\left|\frac{3}{2},+\frac{1}{2}\right\rangle &= -\frac{1}{\sqrt{6}}(X+\mathrm{i}Y)|\downarrow\rangle + \sqrt{\frac{2}{3}}Z|\uparrow\rangle \\
\left|\frac{3}{2},-\frac{3}{2}\right\rangle &= \frac{1}{\sqrt{2}}(X-\mathrm{i}Y)|\downarrow\rangle
\end{aligned} \tag{5}$$

where X, Y and Z being functions which transform in the same way as the atomic x-, y-, z-functions under the symmetry operations which map the local tetrahedron onto itself.

To proceed, we discuss first the eigenvalues and eigenfunctions of equation (1) for the bulk situation $V(z) \equiv 0$, as these solutions will be the basis for the problem with a potential barrier or well along z.

(a) *Bulk solutions* As result of the translational symmetry along z, the envelope function along this direction is also a plane wave with wave vector k_z, and consequently the operator $\hat{k}_z$ in equation (2) becomes just a number (k_z).

From the diagonalization of each 2×2 block of equation (1) we obtain the well-known bulk dispersion relation for the valence band in III–V compound semiconductors [22]:

$$E(k) = Ak^2 \pm \left[B^2k^4 + C^2(k_x^2k_y^2 + k_y^2k_z^2 + k_x^2k_z^2)\right]^{1/2} \tag{6}$$

where $A = (\hbar^2/2m)\gamma_1$, $B = (\hbar^2/m)\gamma_2$, $C^2 = (3\hbar^4/m^2)(\gamma_3^2 - \gamma_2^2)$, $k^2 = k_x^2 + k_y^2 + k_z^2$ and the $+$ $(-)$ sign refers to light (heavy) holes; each eigenvalue is twice degenerate, as a result of time-reversal and inversion symmetry. As will become clear below, the magnitude of interest to us is k_z as a function of E (for a given k_x and k_y); from equation (6) we easily obtain

$$\begin{aligned}
k_z^2(k_x, E) = \frac{1}{(A^2 - B^2)} \Bigg\{ & AE - \left(A^2 - B^2 - \frac{C^2}{2}\right)k_x^2 \\
& \mp \left[B^2E^2 + AC^2Ek_x^2 - C^2\left(A^2 - B^2 - \frac{C^2}{4}\right)k_x^4\right]^{1/2} \Bigg\}
\end{aligned} \tag{7}$$

where the $-$ $(+)$ sign corresponds to light (heavy) holes and we set $k_y = 0$ for simplicity. A graphical representation of this equation using Luttinger parameters corresponding to GaAs is given in figure 1 for heavy holes (HH) and figure 2 for light holes (LH), for a typical value of $k_x = 6 \times 10^{-2}(2\pi/a)$; corresponding numerical values are given in table 1. As these dispersion relations will be the basis for our interpretation of the reflection and transmission coefficients, they deserve a few comments, which we will now list.

(i) There are two critical energies E_h^- (> 0) and E_m (< 0). If $E < E_m$ both solutions of k_z are pure imaginary, with the absolute value of the LH solution being smaller than that of the HH solution: $|k_z^{(L)}| < |k_z^{(H)}|$; in the limit $E \to -\infty$, $k_z^{(L)} \to \pm i\sqrt{-E/(A+B)}$, while $k_z^{(h)} \to \pm i\sqrt{-E/(A-B)}$. For energies in the range $E_m < E < E_h^-$, both solutions

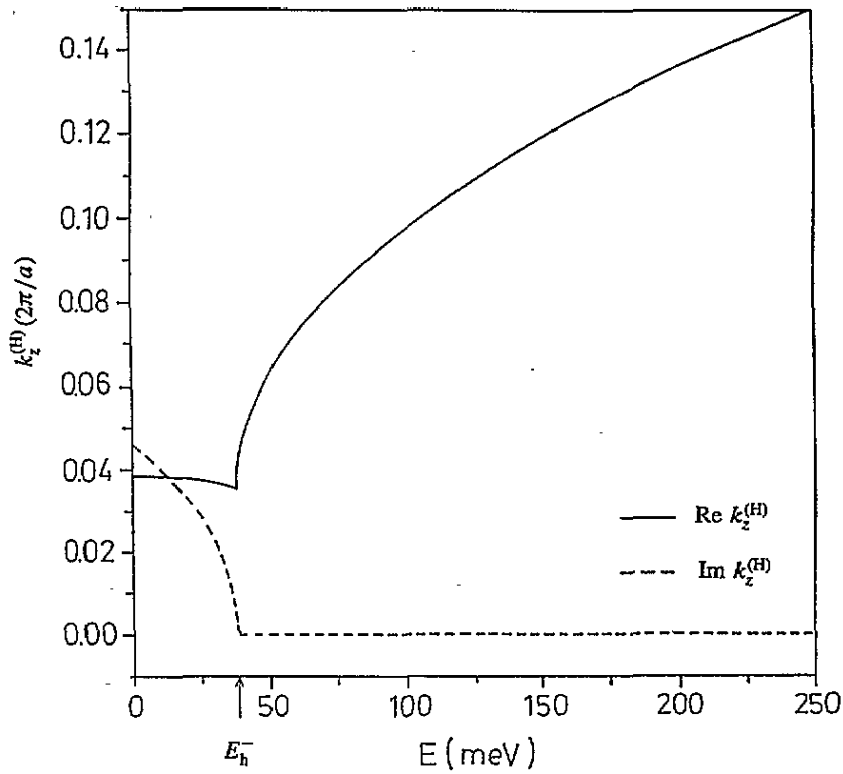

Figure 1. Bulk GaAs real and imaginary components of the heavy-hole wave number $k_z^{(H)}$ as a function of energy; the origin of energy is at the top of the valence band, and $k_x = 6 \times 10^{-2}(2\pi/a)$. Propagating states are allowed when $E > E_h^-$.

of k_z are complex, with real and imaginary non-vanishing components. A simple analysis of equation (7) shows that in this case the real and imaginary parts of $k_z^{(L)}$ and $k_z^{(H)}$ should fulfil the conditions $\mathrm{Re}\, k_z^{(H)} = \mp \mathrm{Re}\, k_z^{(L)}$ and $\mathrm{Im}\, k_z^{(H)} = \pm \mathrm{Im}\, k_z^{(L)}$; as can be seen in figures 1 and 2, we have chosen to have equal (unequal) signs for the imaginary (real) component. Mathematically, these latter solutions arise when the argument inside the square root in equation (7) is negative, and from the condition that the argument be zero we obtain

$$E_m = \Gamma^- \frac{\hbar^2 k_x^2}{2m} \qquad E_h^- = \Gamma^+ \frac{\hbar^2 k_x^2}{2m} \tag{8}$$

where

$$\Gamma^{\pm} = \frac{3}{2}\frac{\gamma_1(\gamma_3^2 - \gamma_2^2)}{\gamma_2^2}\left\{-1 \pm \left[1 + \frac{4}{3}\frac{\gamma_2^2}{\gamma_1^2(\gamma_3^2 - \gamma_2^2)}(\gamma_1^2 - \gamma_2^2 - 3\gamma_3^2)\right]^{1/2}\right\}.$$

Both types of solutions (pure imaginary and complex), while unphysical in a bulk situation, should be considered in the present problem, as they are physically acceptable solutions for finite regions such as barriers and wells.

(ii) For $E > E_h^-$, the HH solution is real; the same is true for the LH when $E > E_l$. Imposing the condition $k_z = 0$ on equation (7) we obtain two solutions:

$$E_l = (\gamma_1 + 2\gamma_2)\frac{\hbar^2 k_x^2}{2m} \tag{9}$$

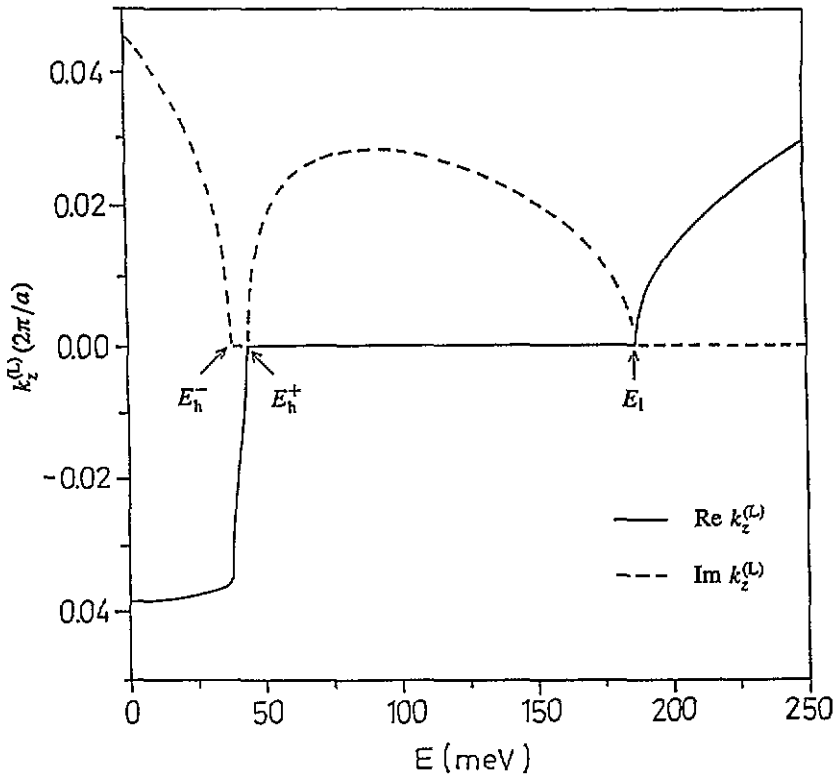

Figure 2. *Bulk GaAs real and imaginary components of the light-hole wave number* $k_z^{(L)}$ *as a function of energy;* $E = 0$ *corresponds to the top of the valence band, and* $k_x = 6 \times 10^{-2}(2\pi/a)$. *Propagating states are allowed when* $E > E_l$ *and in the window between* E_h^- *and* E_h^+.

and

$$E_h^+ = (\gamma_1 - 2\gamma_2)\frac{\hbar^2 k_x^2}{2m}. \tag{10}$$

The significance of these two energies is that $k_z^{(L)}$ becomes pure imaginary when $E_h^+ < E < E_l$, while it is real in the window $E_h^- < E < E_h^+$. Some words are in order concerning this classification of solutions as heavy or light. While the distinction is clear for energies $E > E_l$, as $E - A(k_x^2 + k_z^2)$ (see equation (6)) is positive for $k_z^{(L)}$ and negative for $k_z^{(H)}$, it becomes more complicated at lower energies. By following the sign of the function $E - A(k_x^2 + k_z^{(L)2})$ for decreasing values of E ($E < E_l$), it is seen that the pure imaginary solution $k_z^{(L)}$ evolves progressively towards a pure imaginary HH solution, and when $E_h^- < E < E_h^+$ in a propagating HH solution. That is, the solution that by convenience we call light in figure 2 is actually of heavy type below some threshold energy between E_h^+ and E_l.

The eigenvectors associated with the eigenvalues (6) are

$$\psi_{HH}^U(r) = \begin{pmatrix} F_{1H} \\ F_{2H} \\ 0 \\ 0 \end{pmatrix} e^{ik\cdot r} \qquad \psi_{LH}^U(r) = \begin{pmatrix} F_{1L} \\ F_{2L} \\ 0 \\ 0 \end{pmatrix} e^{ik\cdot r} \tag{11a}$$

$$\psi^{\mathrm{L}}_{\mathrm{HH}}(r) = \begin{pmatrix} 0 \\ 0 \\ F^{\dagger}_{2\mathrm{H}} \\ F_{1h} \end{pmatrix} \mathrm{e}^{\mathrm{i}k\cdot r} \qquad \psi^{\mathrm{L}}_{\mathrm{LH}}(r) = \begin{pmatrix} 0 \\ 0 \\ F_{2\mathrm{L}} \\ F^{\dagger}_{1\mathrm{L}} \end{pmatrix} \mathrm{e}^{\mathrm{i}k\cdot r} \tag{11b}$$

where $F_{1\mathrm{H}} = (P-Q-E)/N_{\mathrm{H}}$, $F_{2\mathrm{H}} = -\tilde{R}^{\dagger}/N_{\mathrm{H}}$, $F_{1\mathrm{L}} = \tilde{R}/N_{\mathrm{L}}$, $F_{2\mathrm{L}} = (E-P-Q)/N_{\mathrm{L}}$, and $N_{\mathrm{H}} = (|P-Q-E|^2+|\tilde{R}|^2)^{1/2}$, $N_{\mathrm{L}} = (|E-P-Q|^2+|\tilde{R}|^2)^{1/2}$ are normalization constants. While the eigenvector notation as a four-component vector is redundant, its usefulness will be clear in the next section, where the symmetry properties of the Hamiltonian will be analysed.

Both for checking the consistency of the boundary conditions across each interface and for the calculation of the reflection and transmission coefficients we need an explicit expression for the probability current in a multiband situation within the effective-mass approximation. As this has been already discussed elsewhere [23], we just quote the result for the probability current density along z:

$$j_{z,n} = \mathrm{Re}\frac{\hbar}{m}\left\{\left[\gamma_1(|F_{1n}|^2+|F_{2n}|^2) - 2\gamma_2(|F_{1n}|^2-|F_{2n}|^2)\right]k_z^{(n)} + \mathrm{i}\,2\sqrt{3}\gamma_3 F_{1n}F^{*}_{2n}k_x\right\} \tag{12}$$

with $n = \mathrm{H,L}$.

Moreover, as for the calculation of the scattering coefficients we will evaluate the probability current density at the asymptotic semi-infinite regions $z \to \pm\infty$, only real values of $k_z^{(\mathrm{H})}$ and $k_z^{(\mathrm{L})}$ are allowed in equation (12), corresponding to propagating states. Under this condition, the expression simplifies considerably [12]:

$$j_{z,n} = \frac{\hbar}{m}k_z^{(n)}\left[\frac{(\gamma_1^2+2\gamma_2^2-6\gamma_3^2)k_x^2+(\gamma_1^2-4\gamma_2^2)(k_z^{(n)})^2-2m\gamma_1 E/\hbar^2}{\gamma_1 k^2 - 2mE/\hbar^2}\right]. \tag{13}$$

For the simplest case $k_x = 0$, $k_z^{(\mathrm{H})} = k_z^{(\mathrm{L})} = k_z$, and equation (13) reduces to

$$j_{z,\mathrm{H}} = \frac{\hbar}{m}(\gamma_1 - 2\gamma_2)k_z$$

$$j_{z,\mathrm{L}} = \frac{\hbar}{m}(\gamma_1 + 2\gamma_2)k_z$$

which is the usual result for particles with parabolic and isotropic dispersion relations. Note that when $k_x = k_y = 0$, all the off-diagonal terms in the block-diagonalized Luttinger Hamiltonian vanish, and what remains are the diagonal terms with electron-like kinetic energy and effective-masses $m/(\gamma_1 - 2\gamma_2)$ (heavy hole) and $m/(\gamma_1 + 2\gamma_2)$ (light hole).

Real positive (negative) values of $k_z^{(n)}$ correspond to right- (left-) propagating holes; following the notation of [12] we will denote the current associated with the right- (left-) propagating states as $j_{z,n}$ ($j_{-z,n}$); from equation (13) it can be seen that $j_{z,n} = -j_{-z,n}$.

(b) *Heterojunction solutions.* As the presence of interfaces along z breaks the translational symmetry in this direction, plane waves with k_z become mixed with $-k_z$, while k_x and k_y remain good quantum numbers. Accordingly, the more general upper-block wave function corresponding to the semi-infinite layer to the left of the barrier or well is given by a linear combination of heavy- and light-hole states moving in both directions along z:

$$\psi^{\mathrm{U}}_{\mathrm{left}}(r) = \mathrm{e}^{\mathrm{i}k_x x}\left[a\begin{pmatrix} F_{1\mathrm{H}} \\ F_{2\mathrm{H}} \\ 0 \\ 0 \end{pmatrix}\mathrm{e}^{\mathrm{i}k_z^{(\mathrm{H})}z} + c\begin{pmatrix} F_{1\mathrm{L}} \\ F_{2\mathrm{L}} \\ 0 \\ 0 \end{pmatrix}\mathrm{e}^{\mathrm{i}k_z^{(\mathrm{L})}z}\right.$$

$$+b\begin{pmatrix} F_{1H} \\ F_{2H}^{-} \\ 0 \\ 0 \end{pmatrix} e^{-ik_z^{(H)}z} + d\begin{pmatrix} F_{1l}^{-} \\ F_{2L} \\ 0 \\ 0 \end{pmatrix} e^{-ik_z^{(L)}z} \Bigg] \tag{14a}$$

where a and c are amplitude probabilities for left-incident heavy and light holes, while b and d are the corresponding reflection amplitudes; $k_z^{(H)}$ and $k_z^{(L)}$ are the HH and LH solutions of equation (7) for a given k_x and energy E, $F_{2H}^{-} = F_{2H}(-k_z^{(H)})$ and $F_{1L}^{-} = F_{1L}(-k_z^{(L)})$.

The associated solution in the barrier or well intermediate region is

$$\psi_{int}^{U}(r) = e^{ik_x x}\Bigg[\alpha\begin{pmatrix} \bar{F}_{1H} \\ \bar{F}_{2H} \\ 0 \\ 0 \end{pmatrix} e^{i\bar{k}_z^{(H)}z} + \beta\begin{pmatrix} \bar{F}_{1L} \\ \bar{F}_{2L} \\ 0 \\ 0 \end{pmatrix} e^{i\bar{k}_z^{(L)}z}$$
$$+\gamma\begin{pmatrix} \bar{F}_{1H} \\ \bar{F}_{2H}^{-} \\ 0 \\ 0 \end{pmatrix} e^{-i\bar{k}_z^{(H)}z} + \delta\begin{pmatrix} \bar{F}_{1L}^{-} \\ \bar{F}_{2L} \\ 0 \\ 0 \end{pmatrix} e^{-i\bar{k}_z^{(L)}z}\Bigg] \tag{14b}$$

with $\bar{F}$ and $\bar{k}_z$ denoting magnitudes evaluated at the barrier or well region.

Finally, the solution at the right semi-infinite layer is given by

$$\psi_{right}^{U}(r) = e^{ik_x x}\Bigg[e\begin{pmatrix} F_{1H} \\ F_{2H} \\ 0 \\ 0 \end{pmatrix} e^{ik_z^{(H)}z} + g\begin{pmatrix} F_{1L} \\ F_{2L} \\ 0 \\ 0 \end{pmatrix} e^{ik_z^{(L)}z}$$
$$+f\begin{pmatrix} F_{1H} \\ F_{2H}^{-} \\ 0 \\ 0 \end{pmatrix} e^{-ik_z^{(H)}z} + h\begin{pmatrix} F_{1L}^{-} \\ F_{2L} \\ 0 \\ 0 \end{pmatrix} e^{-ik_z^{(L)}z}\Bigg] \tag{14c}$$

with e and g being transmission amplitudes, and f, h right-incident amplitudes. A trivial generalization (using (11b)) gives a similar set of solutions corresponding to the lower block of equation (1).

Once interfaces between two semiconductor materials along z are allowed, the question about the boundary conditions naturally arises; besides the continuity of the envelope function at each heterointerface, a second set of boundary conditions is obtained by integrating equation (1) between $z_0 - \epsilon$ and $z_0 + \epsilon$ with z_0 the interface coordinate, and taking the limit $\epsilon \to 0$ ($\epsilon > 0$) [10]. The explicit expression for the resulting boundary matrix can be found elsewhere [23]; it is quite reassuring that this procedure is consistent with the requirement that the probability current density given by equation (12) be constant along z. Application of these boundary conditions to both interfaces at $z = 0$ and $z = L$ yields a homogeneous system of eight linear equations (four at each interface) for the twelve unknowns $a, b, c, d, \alpha, \beta, \gamma, \delta, e, f, g$ and h. In order to have a mathematically well-defined problem we should take, for example, $a = 1$ and $c = f = h = 0$ in equation (14), which amounts to limiting ourselves to the case of an incident HH coming from $z = -\infty$. As a result of this simplification we obtain an inhomogeneous system of eight linear equations whose solution can be found numerically; the corresponding results will be given in the next section.

Assuming that we have found these eight amplitude probabilities, the next step is the calculation of the reflection and transmission probabilities. Let us define the reflectivity for

the heavy hole R_{HH} and for the light hole R_{LH} as

$$R_{HH} = -\frac{|b|^2 j_{-z,H}}{j_{z,H}} = |b|^2 \tag{15}$$

and

$$R_{LH} = -\frac{|d|^2 j_{-z,L}}{j_{z,H}} = \frac{|d|^2 j_{z,L}}{j_{z,H}} \tag{16}$$

respectively. The transmissivities T_{HH} and T_{LH} are defined in an analogous way:

$$T_{HH} = \frac{|e|^2 j_{z,H}}{j_{z,H}} = |e|^2 \tag{17}$$

$$T_{LH} = \frac{|g|^2 j_{z,L}}{j_{z,H}} \tag{18}$$

while the conservation of current requires $R_{HH} + R_{LH} + T_{HH} + T_{LH} = 1$, which is a very useful relation for checking the accuracy of the numerical results.

Table 1. Material parameters and critical energies (in meV) for several values of k_x (in units of $2\pi/a$, where $a = 5.65$ Å is the lattice constant of GaAs). The Luttinger parameters $\gamma_1, \gamma_2, \gamma_3$ for GaAs and AlAs have been taken from [25]; the corresponding values for the alloy $Al_{0.3}Ga_{0.7}As$ were obtained by linear interpolation. The parameters Γ^-, Γ^+ are defined in the text. The critical energies E_m, E_h^-, E_h^+ and E_l are measured from the top of the valence band of the corresponding material, and consequently inside the barrier (well) the valence band offset ΔE should be added (subtracted). From [26, 27] $\Delta E(x) = 0.4 \times (1.04x + 0.47x^2)$, which gives $\Delta E = 141.72$ meV for $x = 0.3$.

	Material parameters	GaAs	$Al_{0.3}Ga_{0.7}As$
	γ_1	6.85	5.83
	γ_2	2.1	1.674
	γ_3	2.9	2.417
	Γ^-	−20.89	−21.08
	Γ^+	2.25	2.11
$k_x = 2 \times 10^{-2}$	E_m	−39.33	−39.68
	E_h^-	4.24	3.97
	E_h^+	4.99	4.67
	E_l	20.80	17.28
$k_x = 4 \times 10^{-2}$	E_m	−157.30	−158.73
	E_h^-	16.95	15.88
	E_h^+	19.95	18.69
	E_l	83.21	69.11
$k_x = 6 \times 10^{-2}$	E_m	−353.93	−357.15
	E_h^-	38.14	35.73
	E_h^+	44.90	42.05
	E_l	187.22	155.05

3. Symmetry of the hole scattering matrix

The symmetry properties of the hole reflection and transmission coefficients can be easily formulated using the formalism of the scattering matrix [24]. Figure 3 represents schematically the general problem of two incoming waves (HH and LH) impinging towards

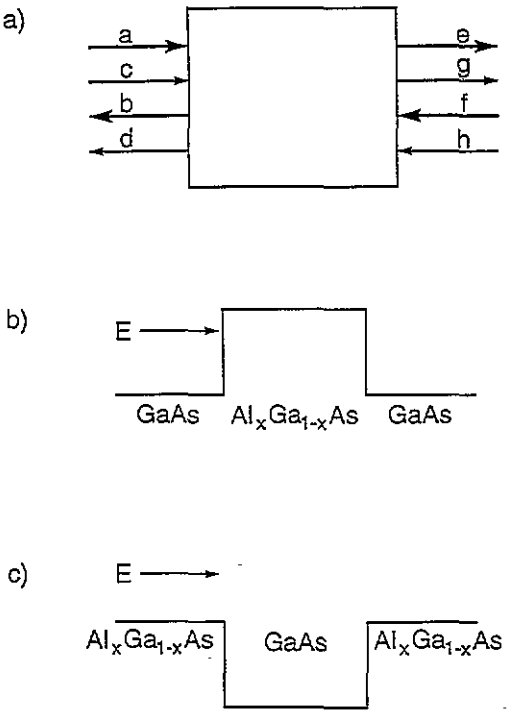

Figure 3. (a) Schematic representation of the problem from a scattering matrix point of view. The square box represents the target (barrier or well), and the arrows the incoming and outgoing probability amplitudes: (b) schematic representation for scattering from a barrier potential; (c) schematic representation for scattering from a well potential.

the target (from the left and right sides), together with the corresponding reflected and transmitted waves.

The scattering matrix **S** is such that applied to the vector I of incoming amplitudes it yields the vector O of outcoming amplitudes

$$O = \mathbf{S}I \tag{19}$$

where

$$\mathbf{S} = \begin{pmatrix} S_{11} & S_{12} & S_{13} & S_{14} \\ S_{21} & S_{22} & S_{23} & S_{24} \\ S_{31} & S_{32} & S_{33} & S_{34} \\ S_{41} & S_{42} & S_{43} & S_{44} \end{pmatrix} \equiv \begin{pmatrix} r_{HH} & r_{HL} & t'_{HH} & t'_{HL} \\ r_{LH} & r_{LL} & t'_{LH} & t'_{LL} \\ t_{HH} & t_{HL} & r'_{HH} & r'_{HL} \\ t_{LH} & t_{LL} & r'_{LH} & r'_{LL} \end{pmatrix} \tag{20}$$

and, using the notation of equations (14*a*) and (14*c*),

$$O = \begin{pmatrix} b \\ d \\ e \\ g \end{pmatrix} \qquad I = \begin{pmatrix} a \\ c \\ f \\ h \end{pmatrix}. \tag{21}$$

The right-hand side of equation (20) represents the scattering matrix in terms of the transmission and reflection amplitudes. To give some examples, r_{HH} represents the amplitude probability that a left-incident HH be reflected as HH, while r'_{LH} corresponds to the amplitude probability that a right-incident HH be reflected as LH. As by conservation of the particle

number, the current density should be the same when evaluated to the left and the right sides of the obstacle, the following equality must be fulfilled:

$$(|a|^2 - |b|^2)j_H + (|c|^2 - |d|^2)j_l = (|e|^2 - |f|^2)j_H + (|g|^2 - |h|^2)j_L \qquad (22)$$

which can be rewritten as

$$|a|^2 j_H + |c|^2 j_L + |f|^2 j_h + |h|^2 j_L = |b|^2 j_H + |d|^2 j_L + |e|^2 j_H + |g|^2 j_L \qquad (23)$$

and, in order to lighten the notation, $j_n \equiv j_{z,n}$. On defining a 4×4 diagonal current matrix

$$\mathbf{J} = \begin{pmatrix} j_H & 0 & 0 & 0 \\ 0 & j_L & 0 & 0 \\ 0 & 0 & j_H & 0 \\ 0 & 0 & 0 & j_L \end{pmatrix} \qquad (24)$$

and two four-component vectors

$$V_O = \mathbf{J}^{1/2} O = \begin{pmatrix} j_H^{1/2} & b \\ j_L^{1/2} & d \\ j_H^{1/2} & e \\ j_L^{1/2} & g \end{pmatrix} \qquad V_I = \mathbf{J}^{1/2} I = \begin{pmatrix} j_H^{1/2} & a \\ j_L^{1/2} & c \\ j_H^{1/2} & f \\ j_L^{1/2} & h \end{pmatrix} \qquad (25)$$

the current-conservation constraint arising from equation (23) can be written in matrix form:

$$V_O^\dagger V_O = V_I^\dagger V_I \qquad (26a)$$

or equivalently

$$O^\dagger \mathbf{J} O = I^\dagger \mathbf{J} I. \qquad (26b)$$

But according to (19) $O = \mathbf{S}I$, $O^\dagger = I^\dagger \mathbf{S}^\dagger$; replacing these two relations in (26) we get $I^\dagger \mathbf{S}^\dagger \mathbf{J} \mathbf{S} I = I^\dagger \mathbf{J} I$, which implies

$$\mathbf{S}^\dagger \mathbf{J} \mathbf{S} = \mathbf{J} \qquad \text{or} \qquad \mathbf{S}^{-1} = \mathbf{J}^{-1} \mathbf{S}^\dagger \mathbf{J} \qquad (27)$$

which is a generalization of the usual unitary condition $\mathbf{S}^{-1} = \mathbf{S}^\dagger$ one gets for electrons from current conservation [24].

The next symmetries to be considered are the ones associated with time-reversal invariance and twofold rotation along the z axis; a related analysis has been carried out in [18] in the original basis of the 4×4 Luttinger Hamiltonian, with the purpose of determining the parity of the bounded-hole solutions of a semiconductor quantum well.

For a system of a single electron the result of Kramers for the time-reversal operator is $K = i\sigma_y K_0$, where σ_y is the y-component of the spin-1/2 Pauli matrices, and K_0 in the Schrödinger representation is the operation of taking the complex conjugate [22]. The Bloch functions X, Y, Z of equation (5) are invariant under K, while $K|\uparrow\rangle = -|\downarrow\rangle$ and $K|\downarrow\rangle = |\uparrow\rangle$.

Acting with the time-reversal operator on the total electronic wave function $\psi(r)$ in equation (3), and using the transformation equations from the set $|J, J_z\rangle$ to the set $|i\rangle$, we obtain for the envelope function

$$\mathbf{K} \begin{pmatrix} F_1(r) \\ F_2(r) \\ F_3(r) \\ F_4(r) \end{pmatrix} = \begin{pmatrix} 0 & 0 & 0 & -1 \\ 0 & 0 & -1 & 0 \\ 0 & 1 & 0 & 0 \\ 1 & 0 & 0 & 0 \end{pmatrix} \mathbf{K}_0 \begin{pmatrix} F_1(r) \\ F_2(r) \\ F_3(r) \\ F_4(r) \end{pmatrix} \qquad (28)$$

which gives the desired expression for $\mathbf{K}$ in the $|i\rangle$ basis.

For zincblende heterojunctions with a [001] growth direction (and, of course, also for the bulk material), a twofold rotation about the growth axis is a symmetry operation. Expressing it as $\mathbf{R} = e^{-i\pi J_z}\mathbf{I}$ and acting on $\psi(r)$ we obtain

$$\mathbf{R}\begin{pmatrix} F_1(x,y,z) \\ F_2(x,y,z) \\ F_3(x,y,z) \\ F_4(x,y,z) \end{pmatrix} = \begin{pmatrix} 0 & 0 & 0 & i \\ 0 & 0 & i & 0 \\ 0 & i & 0 & 0 \\ i & 0 & 0 & 0 \end{pmatrix} \begin{pmatrix} F_1(-x,-y,z) \\ F_2(-x,-y,z) \\ F_3(-x,-y,z) \\ F_4(-x,-y,z) \end{pmatrix}. \tag{29}$$

Note that both $\mathbf{K}$ and $\mathbf{R}$ mix the first two components of the envelope function with the last two; this is the reason for keeping the notation of the eigensolutions as four-component vectors (equation (11)).

The symmetry operation that really is of interest to us is the product $\mathbf{RK}$; from (28) and (29) we obtain

$$\mathbf{RK}\begin{pmatrix} F_1(x,y,z) \\ F_2(x,y,z) \\ F_3(x,y,z) \\ F_4(x,y,z) \end{pmatrix} = \begin{pmatrix} F_1^*(-x,-y,z) \\ F_2^*(-x,-y,z) \\ -F_3^*(-x,-y,z) \\ -F_4^*(-x,-y,z) \end{pmatrix} \tag{30}$$

beyond a global phase factor.

Using this result, application of $\mathbf{RK}$ to states $\psi^{\mathrm{U}}_{\mathrm{left}}(r)$ and $\psi^{\mathrm{U}}_{\mathrm{right}}(r)$ yields

$$\mathbf{RK}\psi^{\mathrm{U}}_{\mathrm{left}}(r) = e^{ik_x x}\left[a^* \begin{pmatrix} F_{1\mathrm{H}} \\ F_{2\mathrm{H}}^- \\ 0 \\ 0 \end{pmatrix} e^{-ik_z^{(\mathrm{H})}z} + c^* \begin{pmatrix} F_{1\mathrm{L}}^- \\ F_{2\mathrm{L}} \\ 0 \\ 0 \end{pmatrix} e^{-ik_z^{(\mathrm{L})}z} + b^* \begin{pmatrix} F_{1\mathrm{H}} \\ F_{2\mathrm{H}} \\ 0 \\ 0 \end{pmatrix} e^{ik_z^{(\mathrm{H})}z} + d^* \begin{pmatrix} F_{1\mathrm{L}} \\ F_{2\mathrm{L}} \\ 0 \\ 0 \end{pmatrix} e^{ik_z^{(\mathrm{L})}z} \right]. \tag{31a}$$

$$\mathbf{RK}\psi^{\mathrm{U}}_{\mathrm{right}}(r) = e^{ik_x x}\left[e^* \begin{pmatrix} F_{1\mathrm{H}} \\ F_{2\mathrm{H}}^- \\ 0 \\ 0 \end{pmatrix} e^{-ik_z^{(\mathrm{H})}z} + g^* \begin{pmatrix} F_{1\mathrm{L}}^- \\ F_{2\mathrm{L}} \\ 0 \\ 0 \end{pmatrix} e^{-ik_z^{(\mathrm{L})}z} + f^* \begin{pmatrix} F_{1\mathrm{H}} \\ F_{2\mathrm{H}} \\ 0 \\ 0 \end{pmatrix} e^{ik_z^{(\mathrm{H})}z} + h^* \begin{pmatrix} F_{1\mathrm{L}} \\ F_{2\mathrm{L}} \\ 0 \\ 0 \end{pmatrix} e^{ik_z^{(\mathrm{L})}z} \right]. \tag{31b}$$

Comparison of this solution with equation (14) shows that effectively the directions of motion along z have been reversed and the amplitude a has been interchanged with b^*, c with d^*, f with e^*, and h with g^*. Hence, as $\mathbf{RK}$ commutes with $\mathbf{H}$, we may make these replacements in equation (19) and obtain the equally valid equation

$$I^* = \mathbf{S}O^*. \tag{32}$$

Equations (19) and (32) can be combined to yield the condition

$$\mathbf{S}^* = \mathbf{S}^{-1} \tag{33}$$

which in conjunction with the pseudo-unitary relation (27) implies the following important property of the hole scattering matrix:

$$\mathbf{S}^\dagger\mathbf{J} = \mathbf{J}\mathbf{S}^*. \tag{34}$$

A straightforward calculation with equation (34) gives the following set of non-trivial relations among the scattering matrix amplitudes:

$$\begin{aligned} &\frac{j_L}{j_H}S_{21} = S_{12} \qquad S_{31} = S_{13} \qquad \frac{j_L}{j_H}S_{41} = S_{14} \\ &\frac{j_H}{j_L}S_{32} = S_{23} \qquad S_{42} = S_{24} \qquad \frac{j_L}{j_H}S_{43} = S_{34} \end{aligned} \tag{35}$$

which translate into the following symmetry relations among the reflectivities and transmissivities:

$$\begin{aligned} T_{HH} &= |S_{31}|^2 = |S_{13}|^2 = T'_{HH} \\ T_{LL} &= |S_{42}|^2 = |S_{24}|^2 = T'_{LL} \\ T_{LH} &= \frac{j_L}{j_H}|S_{41}|^2 = \frac{j_H}{j_L}|S_{14}|^2 = T'_{HL} \\ T_{HL} &= \frac{j_H}{j_L}|S_{32}|^2 = \frac{j_L}{j_H}|S_{23}|^2 = T'_{LH} \\ R_{LH} &= \frac{j_L}{j_H}|S_{21}|^2 = \frac{j_H}{j_L}|S_{12}|^2 = R_{HL} \\ R'_{LH} &= \frac{j_L}{j_H}|S_{43}|^2 = \frac{j_H}{j_L}|S_{34}|^2 = R'_{HL}. \end{aligned} \tag{36}$$

It is important to note that the validity of these symmetry relations goes beyond in the particular case of a single barrier, as it is clear from the derivation that they should be fulfilled in any scattering process to which the schematic representation of figure 3 applies—the square box being a single barrier or well, a double-barrier tunnelling system, a superlattice, etc.

Using similar procedures, it is easy to see that as a result of the inversion symmetry of the Luttinger Hamiltonian in equation (1), the problem of a left-incident hole with given amplitude, energy and wave vector k, is equivalent to the problem of the same hole coming from the right, with the same amplitude and energy but the opposite sign of k. Note that inversion is not a symmetry operation of the zincblende crystal structure; however, it is a good symmetry operation of the Hamiltonian given by equation (1), because we have neglected k-linear terms.

4. Numerical results

Under the conditions explained above (for instance, $a = 1, c = h = f = 0$) the task of finding the transmission and reflection coefficients amounts to solving numerically an inhomogeneous linear system of eight equations. We present in this section some results of these calculations for barrier and well geometries; unless stated otherwise, L (barrier or well size) = 50 Å, $\Delta E = 141.72$ meV (corresponding to an Al mole fraction $x = 0.3$) and $k_x = 2 \times 10^{-2}(2\pi/a)$. Values of the remaining material parameters are given in table 1.

(a) *Scattering from a barrier potential (figure 3(b)).* We display in figure 4 the energy-dependent reflectivities and transmissivities corresponding to the case of a HH impinging from the left on a $Al_{0.3}Ga_{0.7}As$ barrier. As expected, for energies much smaller than the barrier height, the reflectivities are close to unity while the transmissivities are close to zero. According to table 1, for $E < E_l(\text{GaAs}) \simeq 21$ meV no reflection or transmission of LH is possible, and consequently $R_{HH} \simeq 1$. At $E = E_l(\text{GaAs})$ the light-hole channel

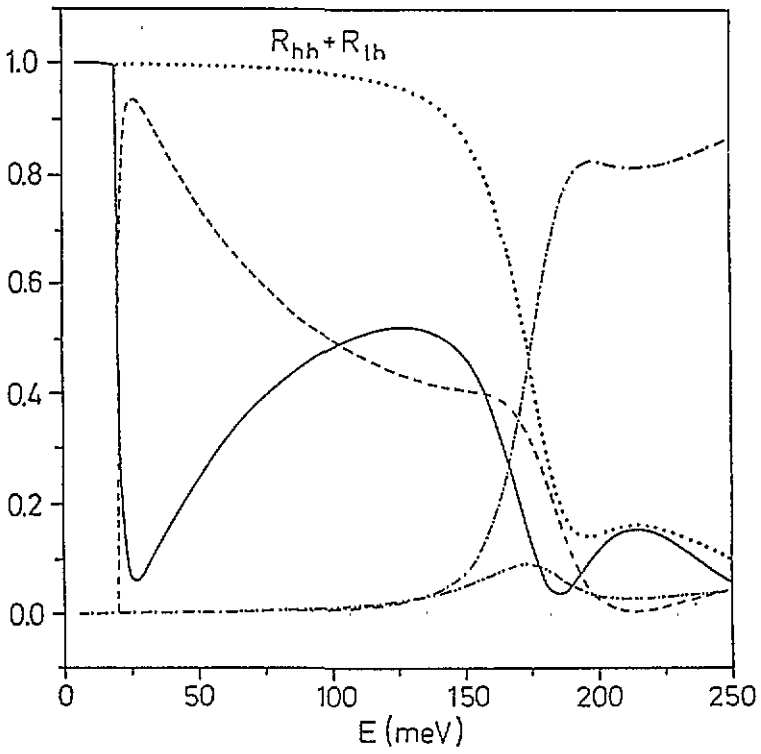

Figure 4. Reflectivities and transmissivities corresponding to a heavy hole impinging on a barrier from the left. The origin of energy has been taken at the top of the GaAs valence band, $L = 50$ Å and $k_x = 2 \times 10^{-2}(2\pi/a)$. Key: ···, $R_{HH} + R_{LH}$; —, R_{HH}; - - -, R_{LH}; ·····, T_{HH}; ·····, T_{LH}.

opens for reflection (and transmission), and accordingly the off-diagonal reflectivity R_{LH} rises abruptly (as in this regime $R_{HH} \simeq 1 - R_{LH}$, the diagonal reflectivity has a strong decrease). While this behaviour of reflectivities that increase with energy (for energies below the barrier threshold) contradicts what one intuitively expects, the total reflectivity $R_{HH} + R_{LH}$ decreases when the energy increases, as expected. The abrupt change in R_{HH} and R_{LH} can be understood qualitatively in the following way: when $E \ll \Delta E$ the barrier behaves as a strong scattering centre, and one should expect considerable reflection and heavy–light-hole mixing effects. While the former effect is evident for $E < E_1(\text{GaAs})$, the mixing reveals abruptly for energies slightly larger than this energy, as in this regime one expects both R_{HH} and R_{LH} to be of the same order of magnitude. A more quantitative analysis is possible by assuming that when $E \ll \Delta E$, the barrier is equivalent to an infinitely high potential step. Analytic solutions for R_{HH} and R_{LH} are available in this case [12]. Expanding these coefficients for energies close to $E_1(\text{GaAs})$ one finds, for instance, that $R_{HH}(E_1 + \varepsilon) \simeq 1 - \eta\sqrt{\varepsilon}$ ($\varepsilon \to 0^+$, η being an energy-independent coefficient), which explains the infinite slope in R_{HH} and R_{LH} when the LH channel opens for reflection. The next interesting feature of figure 4 happens at $E = E_h^-(Al_{0.3}Ga_{0.7}As) + \Delta E \simeq 146$ meV, where the HH channel in the barrier opens for transmission and consequently T_{HH} starts to rise. Similarly, at $E = E_1(Al_{0.3}Ga_{0.7}As) + \Delta E \simeq 159$ meV the LH channel opens, and T_{LH} increases; the increase of the transmissivities is followed by a decrease of the reflectivities. Note that for $E \simeq 215$ meV the total reflectivity (transmissivity)

$R_{HH} + R_{LH}$ ($T_{HH} + T_{LH}$) shows a weak increase (decrease); this is associated with the building of a very primitive above-the-barrier resonant state. While electrons have an infinite number of above-the-barrier resonant energies, where the transmissivity equals unity and reflectivity zero, we have found that the equivalent effect for the holes, due to the mixing at $k_x \neq 0$, only exists for very special choices of the parameters involved. As expected, at even larger energies, all the reflectivities and off-diagonal transmissivity tend to zero, the only survival being the diagonal transmissivity R_{HH}, as mixing and reflection barrier effects become progressively less important.

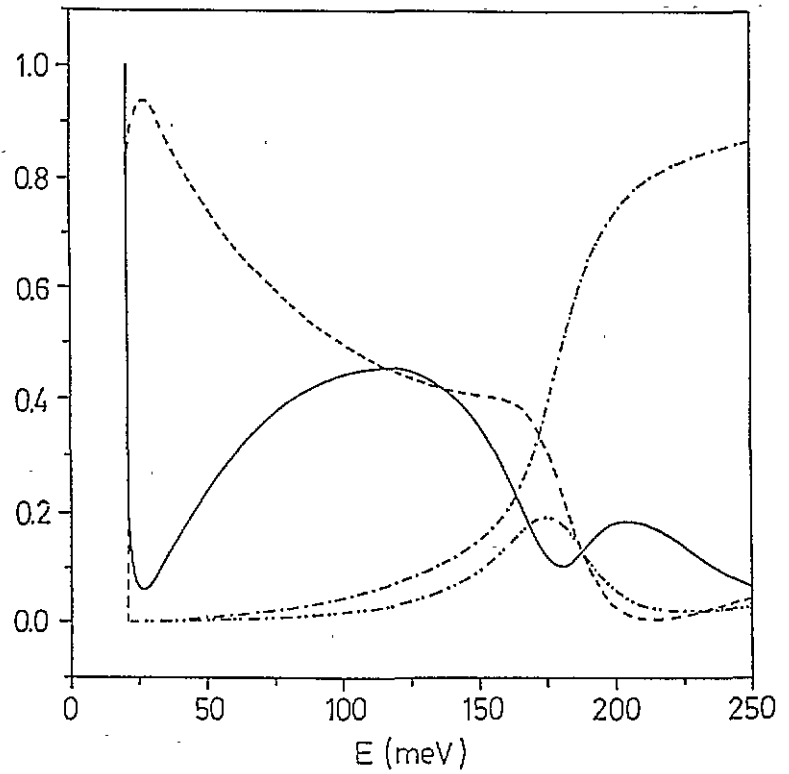

Figure 5. As figure 4, but for an impinging light hole. Key: —, R_{LL}; - - -, R_{HL}; ·····, T_{LL}; ·-·-·-, T_{HL}

Figure 5, corresponding to a LH impinging from the left ($c = 1, a = f = h = 0$) on the same barrier as shown in figure 4, while it is qualitatively similar to the previous figure (under the L $\leftrightarrow$ H change), shows some differences, detailed below

(i) The threshold energy for propagation of a LH state in the left region is given by $E_l(\text{GaAs}) \simeq 21$ meV, and not $E_h^-(\text{GaAs}) \simeq 4$ meV, as corresponds to the HH propagation of figure 4.

(ii) While for the case of an impinging HH both the diagonal and off-diagonal transmissivities T_{HH} and T_{LH} are essentially zero for energies below the critical barrier values $E_h^-(Al_{0.3}Ga_{0.7}As) + \Delta E$ and $E_l(Al_{0.3}Ga_{0.7}As) + \Delta E$, respectively, the corresponding magnitudes T_{LL} and T_{HL} are sizable almost as soon as the LH channel is open for incidence in the GaAs semi-infinite regions. That means that the barrier is more 'transparent' for tunnelling of LH than for tunnelling of HH, which is reminiscent of the situation for $k_x = 0$. This is easily understood by recalling that for $E < E_m(Al_{0.3}Ga_{0.7}As) + \Delta E$, $k_z^{(H)}$ and $k_z^{(L)}$ in

the barrier material are pure imaginary and obey the condition $|k_z^{(L)}| < |k_z^{(H)}|$. This means that the decay length of the LH solution through the barrier is smaller than the decay length of the HH solution, and consequently its transmissivity is bigger.

From the comparison of figures 4 and 5 it is important to note the equality $R_{LH} = R_{HL}$, as required by the symmetries of the hole scattering matrix given at the end of the previous section. It is also worth commenting on the lack of any above-barrier oscillation in the diagonal transmissivity T_{LL}. This is related to the fact that for $E > E_l(Al_{0.3}Ga_{0.7}As) + \Delta E$, both $k_z^{(H)}$ and $k_z^{(L)}$ are real and such that $|k_z^{(H)}| > |k_z^{(L)}|$. Consequently, the condition $k_z L \simeq 1$ is reached earlier for HH than for LH, and the oscillations are absent in the latter case (they appear, however, at higher energies).

As a check of the symmetry relations, we present in figure 6 the reflectivities and transmissivities associated with a right-incident HH ($f = 1, a = c = h = 0$); comparison with figures 4 and 5 yields the equalities $T_{HH} = T'_{HH}, T_{HL} = T'_{LH}$, as required by equation (36).

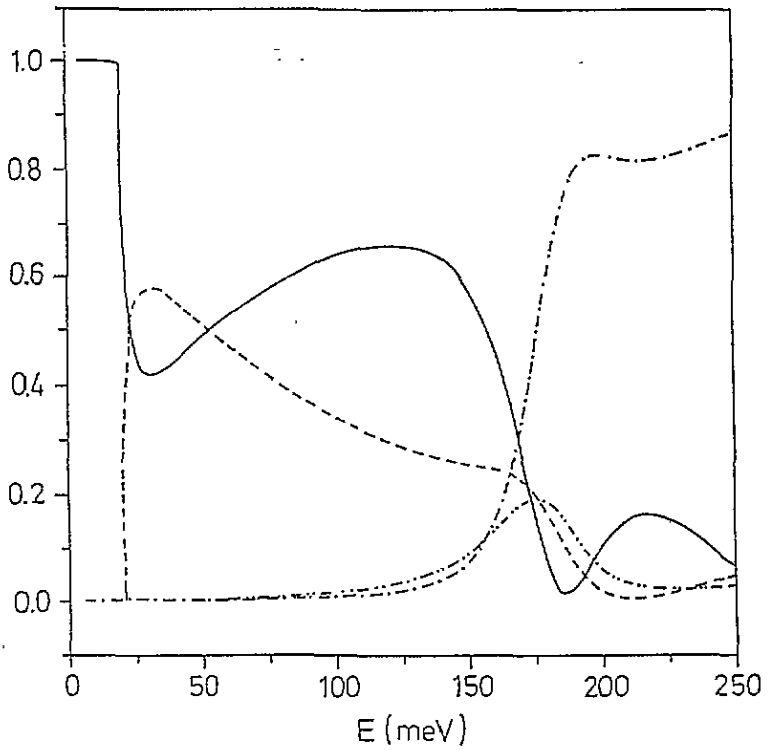

Figure 6. As figure 4, but for a heavy hole impinging from the right. Key: —, R'_{HH}; - - -, R'_{LH}; ·····, T'_{HH}; ·····, T'_{LH}.

(b) *Scattering from a well potential (figure 3(c)).*

Turning now to the well configuration, where the GaAs and $Al_{0.3}Ga_{0.7}As$ materials are interchanged, we display in figure 7 the reflectivities and transmissivities for a HH impinging from the left. The origin of energy has been taken at the bottom of the barrier valence band material, and $k_x = 4 \times 10^{-2}(2\pi/a)$. Our analyses in this configuration are complementary to the results presented in [18], as they study the $E < 0$ quantum-well-bounded solutions, whereas the present results are for the $E > 0$ scattering states.

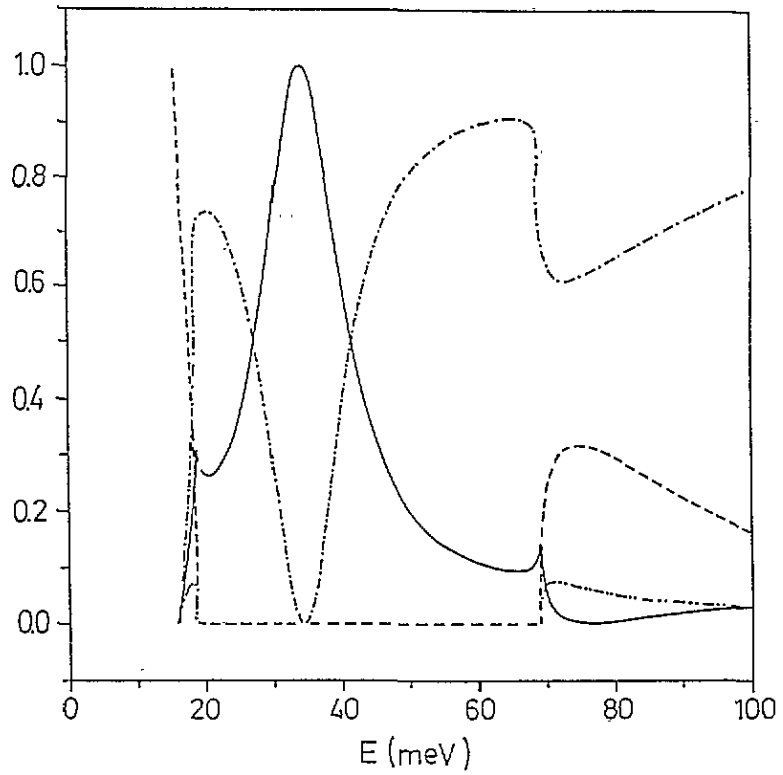

Figure 7. Reflectivities and transmissivities corresponding to a heavy hole impinging towards an $Al_{0.3}Ga_{0.7}As/GaAs/Al_{0.3}Ga_{0.7}$ As quantum well. $E = 0$ corresponds now to the top of the $Al_{0.3}Ga_{0.7}$ As valence band; $L = 50$ Å, and $k_x = 4 \times 10^{-2}(2\pi/a)$. Key: —, R_{HH}; - - -, R_{LH}; ----, T_{HH}; ·····, T_{LH}.

According to table 1, the critical energies corresponding to $Al_{0.3}Ga_{0.7}As$ are $E_h^- \simeq 16$ meV, $E_h^+ \simeq 19$ meV, and $E_l \simeq 69$ meV, while the corresponding values for the well material are at negative energies, and consequently are of no concern to us. Clearly at $E_h^-(Al_{0.3}Ga_{0.7}As)$ both heavy- and light-hole channels open for transmission and reflection, at $E_h^+(Al_{0.3}Ga_{0.7}As)$ the LH channel is not available any more in the semi-infinite-barrier regions, until at $E_l(Al_{0.3}Ga_{0.7}As)$ it is possible again to use this channel for reflection and conduction. This essentially explains the abrupt change of the corresponding reflectivities and transmissivities at these critical energies.

An interesting result is found in the $E_h^+(Al_{0.3}Ga_{0.7}As) < E < E_l(Al_{0.3}Ga_{0.7}As)$ energy range, where the only possibilities for reflection and transmission are the HH states, as for a given $E \simeq 35$ meV, R_{HH} equals exactly unity, and accordingly $T_{HH} = 0$. To understand this at the first sight strange result, it should be realized that for any incident energy inside this window, the LH is quasi-confined while the HH is free. Accordingly, the first presents a quasi-discrete spectrum, degenerate with the continuum of the second. This is reminescent of the problem studied by Fano a long time ago [28], where he finds that resonance/anti-resonance pairs occur whenever a discrete state is coupled to a continuum. Very recently, the same problem was addressed by Boykin *et al* [29], who finds that when a cavity (well) weakly confines one pair of states and strongly confines the other (but with both belonging to a continua), the transmission coefficient for the weakly confined state displays only anti-

resonances, as observed in figure 7. Moreover, a related manifestation of this anti-resonance is the build up of a large density of the strongly confined state in the cavity [29]. This is precisely the behaviour we that found in our system, as can be seen from figure 8, where the sums of the squared moduli of the HH and LH amplitude probabilities in the well are plotted as a function of the incident energy.

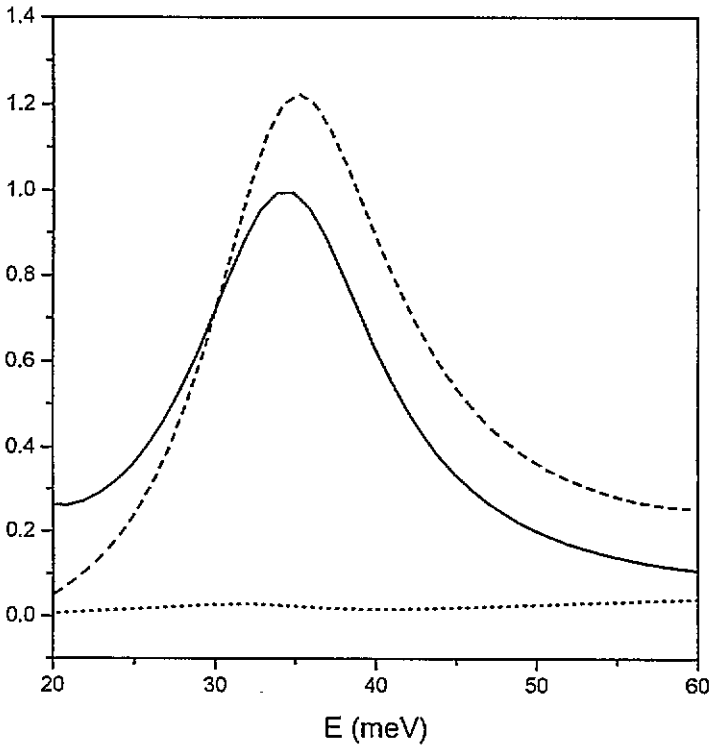

Figure 8. Sums of the squares moduli of the LH (dashed line) and HH (dotted line) probability amplitudes in the well ($|\beta|^2 + |\delta|^2$ and $|\alpha|^2 + |\gamma|^2$, respectively) for the situation of figure 7. The full line corresponds to the diagonal reflectivity R_{HH}.

The equivalent results for a LH impinging from the left are given in figure 9. As the condition to have propagating LH states in the semi-infinite-barrier region implies $E > E_1(Al_{0.3}Ga_{0.7}As)$, all the interesting behaviour of the previous figure is missed. In particular, note the absence of any oscillations in the diagonal transmissivity T_{LL}, which tends asymptotically towards unity for increasing values of the incident LH energy; oscillations are observed, however, at higher incident energies (not shown).

Finally, we consider it instructive to analyse the transition from the finite-barrier case to the simpler limiting case of $L \to \infty$, where the potential along z reduces to a step function; this case was studied in [12]. We display in figure 10 the diagonal reflectivity R_{HH} for a HH impinging from the left, as a function of k_x, and for several barrier sizes; the energy of the incident hole was $E = 100$ meV. For this value of the energy, the LH channel is no longer available for reflection in the GaAs semi-infinite layer for $k_x \geqslant 4.38 \times 10^{-2}(2\pi/a)$ (from equation (9) with $E_1 = E$), and consequently R_{HH} becomes unity for the $L \to \infty$ situation (broken line) at this critical value. However, for any finite value of L, the transmissivity T_{HH} is not exactly zero for k_x larger than this critical value, and accordingly R_{HH} is not unity, as required by the current-conservation sum rule.

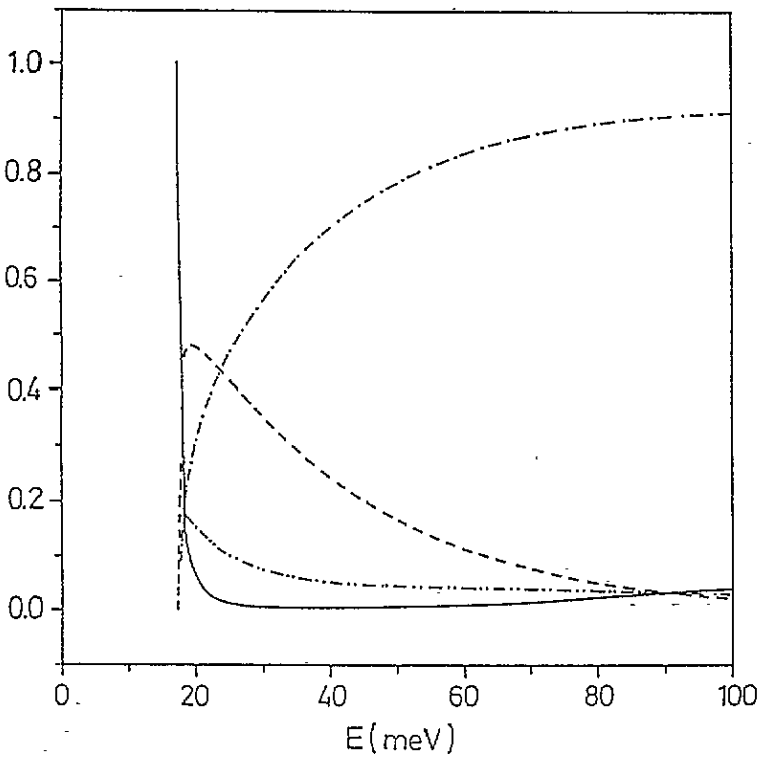

Figure 9. As figure 7, but for an impinging light hole with $k_x = 2 \times 10^{-2}(2\pi/a)$. Key: —, R_{LL}; - - -, R_{HL}; ·····, T_{LL}; ·····, T_{HL}.

5. Conclusions

This work has been devoted to the theoretical study of the quantum mechanical problem of tunnelling and reflection of holes from barriers and wells in semiconductor heterostructures. The calculation has been done within the framework of the envelope-function approach which is based on the effective-mass approximation. By using the Luttinger Hamiltonian to describe the dynamics of holes close at the top of the valence band, we have taken into account exactly the band non-parabolicity, anisotropy, and heavy- and light-hole mixing away from the Brillouin zone centre.

We have worked out the symmetries of the hole scattering matrix which arise as a consequence of time-reversal and spatial invariances; they translate into very general and useful relations among reflectivities and transmissivities.

We also provide a complete set of numerical results concerning the reflection and tunnelling of holes impinging on barriers and wells. A clear interpretation of the results is given in terms of critical energies, where a channel available for conduction disappears (or vice versa), and the remaining coefficients change abruptly as a result of the current-density-conservation constraint.

Contrary to what is found in the electron case, the building of above-the-barrier (or above-the-well) resonant states, with unity transmission coefficient, does not seem to be a general situation away from the zone centre. This is due to the fact that in the presence of HH and LH mixing, the condition for the building of such resonance is much more restrictive than in the case where $k_x = 0$. In contrast, we have found strong anti-resonances for

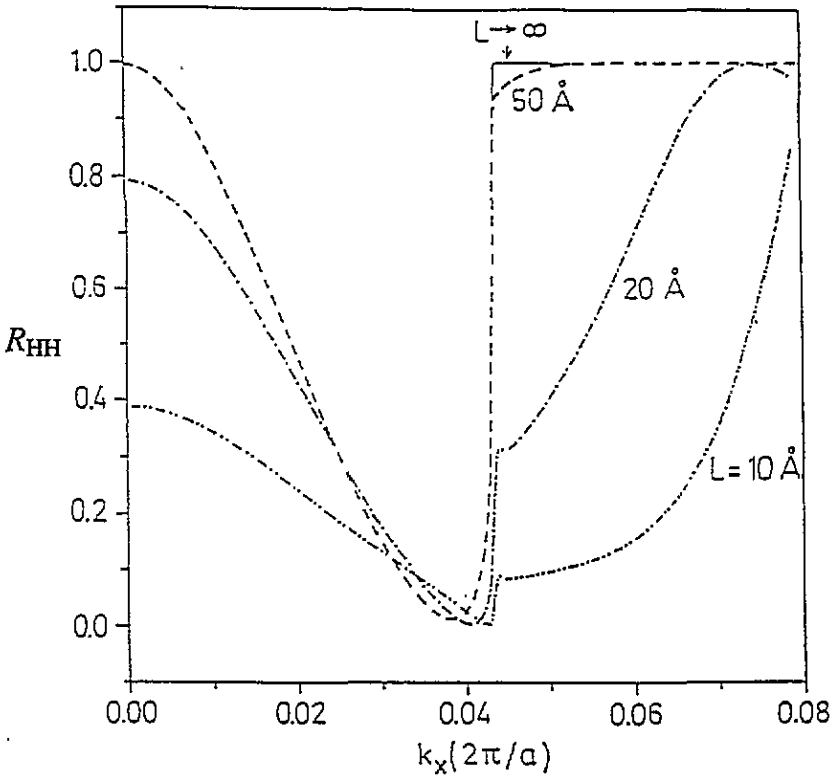

Figure 10. Diagonal reflectivity R_{HH} for a heavy hole impinging towards barriers of several widths from the left. The energy of the incident particle is $E = 100$ meV.

scattering from a well potential, for a situation where the impinging HH is free, while the LH is quasi-confined in the well. This effect, related to a destructive interference between the two coupled channels, is accompanied by a maximum of the LH density in the well. Considered from a broader perspective, beyond the semiconductor condensed-matter framework in which the calculations have been made, the present work is a contribution to the general problem of scattering from a target where mixing among the different channels occurs, restricted to the simplest case of just two possible incoming and outgoing channels.

Acknowledgment

We gratefully acknowledge Veronica Grünfeld for a careful reading of the manuscript.

References

[1] von Klitzing K, Dorda G and Pepper M 1980 *Phys. Rev. Lett.* **45** 494
[2] Tsui D C, Störmer H L and Gossard A C 1982 *Phys. Rev. Lett.* **48** 1559
[3] Mendez E E, Agulló-Rueda F and Hong J M 1988 *Phys. Rev. Lett.* **60** 2426
[4] van Wees B J, van Houten H, Beennakker C W J, Williamson J G, Kouwenhoven L P, Van der Marel D and Foxon C T 1988 *Phys. Rev. Lett.* **60** 848
[5] Wharam D A, Thornton T J, Newbury R, Pepper M, Ahmed H, Frost J E F, Hasko D G, Peacock D C, Ritchie D A and Jones G A C 1988 *J. Phys. C: Solid State Phys.* **21** L209
[6] Smith D L and Mailhiot C 1990 *Rev. Mod. Phys.* **62** 173

[7] Jaros M, Wong K B and Gell M A 1985 *Phys. Rev.* B **31** 1205
[8] Bastard G 1981 *Phys. Rev.* B **24** 5693
[9] White S R and Sham L J 1981 *Phys. Rev. Lett.* **47** 879
[10] Bastard G 1988 *Wave Mechanics Applied to Semiconductor Heterostructures* (Les Ulis: Les Editions de Physique)
[11] Luttinger J M and Kohn W 1955 *Phys. Rev.* **97** 869
[12] Chuang S L 1989 *Phys. Rev.* B **40** 10379
[13] Fu Y, Willander M, Ivchenko E L and Kiselev A A 1993 *Phys. Rev.* B **47** 13498
[14] Ko D Y and Inkson J C 1988 *Semicond. Sci. Technol.* **3** 791; 1988 *Phys. Rev.* B **38** 9945
[15] Brum J A 1991 *Phys. Rev.* B **43** 12082
[16] Ting D Z, Yu E T and McGill T C 1992 *Phys. Rev.* B **45** 3583
[17] Davidovich M A, Anda E V, Tejedor C and Platero G 1993 *Phys. Rev.* B **47** 4475
[18] Andreani L C, Pasquarello A and Bassani F 1987 *Phys. Rev.* B **36** 5887
[19] Wessel R and Altarelli M 1989 *Phys. Rev.* B **39** 10246
[20] Chao C Y-P and Chuang S L 1991 *Phys. Rev.* B **43** 7027
[21] Broido D A and Sham L J 1985 *Phys. Rev.* B **31** 888
[22] Kittel C 1966 *Quantum Theory of Solids* (New York: Wiley)
[23] Altarelli M 1986 *Heterojunctions and Semiconductor Superlattices* ed G Allan, G Bastard, N Boccara and M Voos (Berlin: Springer)
[24] Merzbacher E 1970 *Quantum Mechanics* 2nd edn (New York: Wiley)
[25] *Landolt–Börstein Numerical Data and Functional Relationships in Science and Technology* 1982 Group III, vol 17, ed O Madelung (Berlin: Springer)
[26] Onton A 1973 *Festkörperprobleme XIII (Advances in Solid State Physics)* ed H J Queisser (Braunschweig: Vieweg) p 59
[27] Miller R C, Gossard A C, Kleiman D A and Munteanu O 1984 *Phys. Rev.* B **29** 3740
[28] Fano U 1960 *Phys. Rev.* **124** 1866
[29] Boykin T B, Pezeshki B and Harris J S Jr 1992 *Phys. Rev.* B **46** 12769